

**AN INSTRUMENTATION SYSTEM TO MEASURE IN-SITU
HYDRODYNAMICS DURING BARRIER ISLAND OVERWASH AND
INUNDATION**

An Undergraduate Research Scholars Thesis

by

BRYAN MYRES

Submitted to the Undergraduate Research Scholars program
Texas A&M University
in partial fulfillment of the requirements for the designation as an

UNDERGRADUATE RESEARCH SCHOLAR

Approved by
Research Advisor:

Dr. Jens Figlus

May 2016

Major: Offshore and Coastal Systems Engineering

TABLE OF CONTENTS

	Page
ABSTRACT.....	1
NOMENCLATURE	2
CHAPTER	
I INTRODUCTION	2
Storm regimes	3
Research location and implementation	3
Objective	5
II METHODS	6
Instrument setup and theory	6
Instrument anchoring system	7
III RESULTS & DISCUSSION.....	9
Wave flume testing	9
RBR Pressure/Wave gauge data	11
TCM/Vectrino data	15
IV CONCLUSION.....	21
REFERENCES	22

ABSTRACT

An Instrumentation System to Measure In-situ Hydrodynamics during Barrier Island Overwash and Inundation

Bryan Myres
Department of Offshore and Coastal Systems Engineering
Texas A&M University

Research Advisor: Dr. Jens Figlus
Department of Ocean Engineering

Barrier islands serve as the first line of defense against severe storm events threatening our coastlines and associated infrastructure. The morphology of barrier islands can change dramatically during overtopping and inundation events due to the high-velocity flow and battering waves that attack island features that are typically emergent under normal conditions. The hydrodynamics that occur on a barrier island occurring during these violent events are complex and poorly understood due to the scarcity of field data. The focus of this study is to develop and test an array of low-cost instrument pods that can be rapidly deployed prior to a severe storm event. If successful, these instruments will help further our knowledge of wave overtopping and inundation flow across barrier islands.

CHAPTER I

INTRODUCTION

Storm regimes

According to Sallenger (2000), the impact of storms on coastlines can be described by four different regimes: swash, collision, overwash, and inundation. When a severe storm approaches a barrier island water piles up and creates a storm surge in the direction of the storm's movement. During the swash regime, wave run-up is confined to the foreshore location and does not reach the dunes resulting in zero net movement of sediment to or from the barrier island. As the storm increases in severity, the wave run-up on the barrier island may surpass the base of the foredune ridge, characteristic of the collision regime. In this regime, erosion of the dune toe can take place. Once waves overtop the berm or dune, the barrier island undergoes the overwash regime and net landward transport of sediment occurs. During the most severe conditions, storm surge exceeds the barrier island elevation and the island experiences the inundation regime. Under certain storm conditions and geographical orientations, a fifth regime has been observed when flow is directed offshore, typically during the waning period of the storm. Otherwise known as the storm surge ebb, this regime results in a net sediment flux ocean-ward due to a gradient in water levels between the back-barrier bay and the gulf (Sherwood et al. 2014).

Research location and implementation

Follets Island, a barrier island located along the Upper Texas Coast, is an ideal site to conduct this research due to the island's low elevation and narrow width (approximately 3 feet above sea level and 0.25 miles wide). These factors greatly increase the chance of overwash and

inundation occurring on the island during a storm. To capture the current velocities (magnitude and direction) and water elevation during overwash and inundation events, an array of five instrument pods will be designed, tested, and then deployed pending a severe storm striking the Upper Texas Coast. Each instrument pod will include a co-located tilt current meter and pressure transducer, which will be strategically placed on the barrier island to capture cross-shore and alongshore variations of flow velocities and water depth during an event (Figure 1).

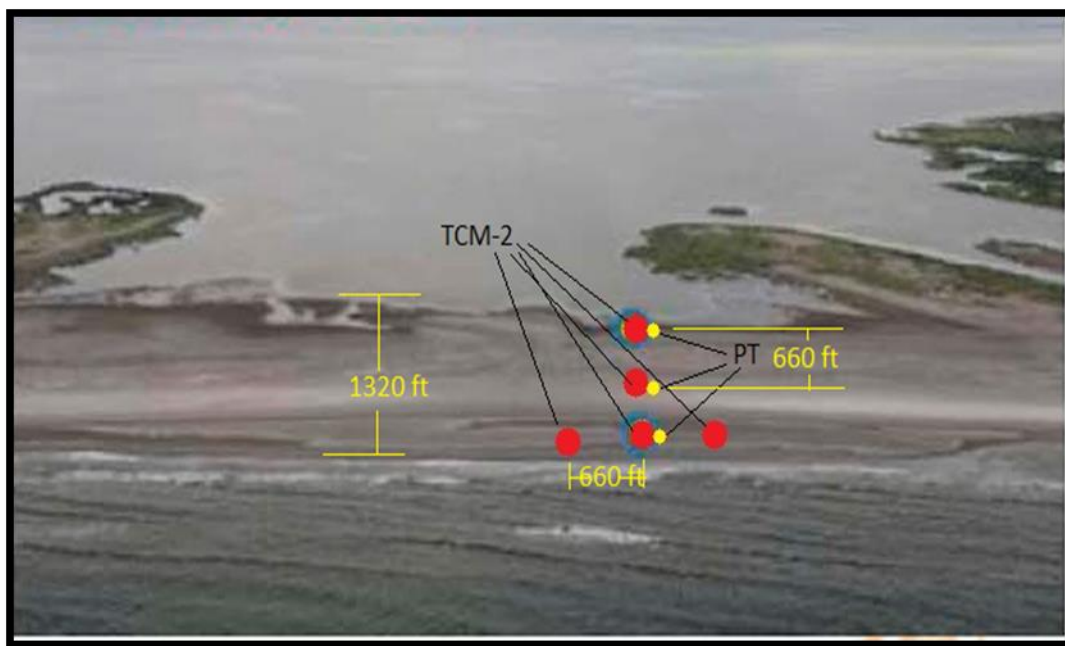


Figure 1. Proposed instrument array setup on Follets Island (Sherwood et al. 2014)

As severe storms are unpredictable and infrequent, this study will focus on instrument setup and calibration as well as lab and field testing of the instrumentation pods. Instrument calibration consists of tuning each instrument in the laboratory to ensure that they are correctly capturing data and therefore will be fully operational when deployed. As a storm approaches, the instruments must be quickly deployed and securely positioned (as in Figure 1) with an anchoring system to ensure the devices hold their location throughout the storm. After the storm passes, the instruments will be retrieved and the data analyzed.

Objective

This study involves the design, testing, and validation of instrumentation pods that are capable of measuring detailed hydrodynamics during extreme event impact on a low-lying barrier island.

The goal is to fully understand and test the sensors in various lab and field conditions to be ready for the next storm that strikes the Upper Texas Coast (Follets Island). While it is understood that such an event cannot be predicted and/or expected to occur during the one-year duration of this project, it is crucial to be prepared and have the instrumentation thoroughly tested before the next event. The proposed research will provide crucial instrumentation design, time-series analysis of pressure, flow magnitude and direction, and validation of the measuring approach for a variety of lab and field settings. The results will help to improve our understanding of barrier island overland flow as well as improve the numerical models that simulate these complex dynamics during storm attack on a barrier island.

CHAPTER II

METHODS

Instrument setup and theory

The instrument pods will feature two instruments: pressure transducers and low-cost tilt-current meters to measure wave action, still-water levels, and current velocity. In addition, the instruments are used in tandem because the tilt current meter must be submerged to function properly and the pressure transducer allows for confirmation of when the water level has surpassed the TCM's minimum depth threshold.

Pressure Transducers

Two brands of pressure transducers, the RBRsolo and HOBO DataLogger, were tested in the flume environment in order to compare data resolution between the two brands and ultimately select the logger that performed the best for use in our pod design. In addition, we were interested in how the sensors behaved when 1) buried in sand, and 2) mounted to the bottom of a concrete pad. To address these questions, we mounted two pressure sensors to a concrete garden block (one from each brand) and then buried the remaining two sensors along either side of the block in the sand.

The pressure transducers utilize the piezo-electric effect meaning that they generate an electric charge in response to applied mechanical stress (change in pressure force). These electrical impulses are recorded by the sensor and converted to pressure using a linear coefficient between the mechanical force and the resulting charge produced. Water surface elevations are calculated from pressure readings using shallow water linear wave theory

$$p = \rho g n \frac{\cosh k(h+z)}{\cosh kh} - \rho g z$$

where the first term represents the dynamic pressure and the second term the hydrostatic pressure. Here, ρ is the density of the fluid, g is the acceleration due to gravity, h is the water depth, k is the wave number, n is the free surface displacement, and z is the depth of the submerged sensor. Solving for water surface elevation (η),

$$\eta = \frac{(p + \rho g z) \cosh kh}{\rho g \cosh k(h+z)}$$

Linear wave theory describes that with increasing water depth, the pressure signature from the dynamic pressure will decrease. Thus, the wave height profile from the pressure plots will be somewhat dampened. These factors will have to be taken into consideration when determining the wave height.

Tilt Current Meter

The TCM-2 tilt current meter (herein referred to as the “TCM”) uses the drag-tilt principle to measure current velocity (Figure 2). In theory, the buoyancy, drag, tether tension, and gravity forces acting on the buoyant logger are in static equilibrium under ideal conditions for constant water velocity.

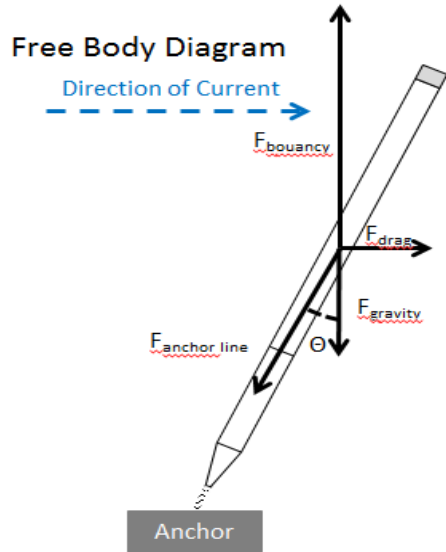


Figure 2. Forces acting on the TCM due to a moving current (Lowell Instruments, 2014)

However, due to non-linearities in the system (e.g. vortex shedding), the TCM is not static and current velocity cannot be obtained directly from a force balance (Lowell Instruments, 2014). Instead, the TCM records the magnitude and direction of tilt imposed by the moving fluid using a 3-axis accelerometer (tilt) and magnetometer (bearing). From static equilibrium, the accelerometer readings are converted to current velocities by applying calibration coefficients embedded in the logger's software derived from laboratory flume and field tests. To filter oscillations due to vortex shedding and the natural frequency of the instrument, Lowell Instruments suggests that data be collected at 16 Hz such that the tilt and bearing can be averaged to 1 Hz.

Instrument anchoring system

In order to capture such violent events as in a hurricane, an anchoring system pod for the instruments was designed to withstand loading from powerful current and wave forcing. Nick Lowell, owner and founder of Lowell Instruments was a huge asset in providing insight on how to secure the instruments to a pod such that data collection was not impeded and probability of

instrument loss was low. The initial instrument pod design is illustrated in Figures 2.1 and 2.2. The pod foundation is a 14'' x 14'' x 3.5'' concrete paving stone with four $\frac{3}{4}$ inch holes drilled in a square pattern near the center (Figure 3b)



Figure 3. (a) Concrete base of the instrument pod (view from above), and (b) TCM mooring system.

The concrete material was selected for the base because of its density, enabling it to remain near the surface of the sand with similar density. This will prevent the system from settling or becoming buried under sand deposits during an inundation event, which would impact instrument performance. The pressure sensor is mounted underneath the paving stone in a protective PVC capsule using pipe clamps and zip ties threaded through the drilled holes seen in Figure 3b.

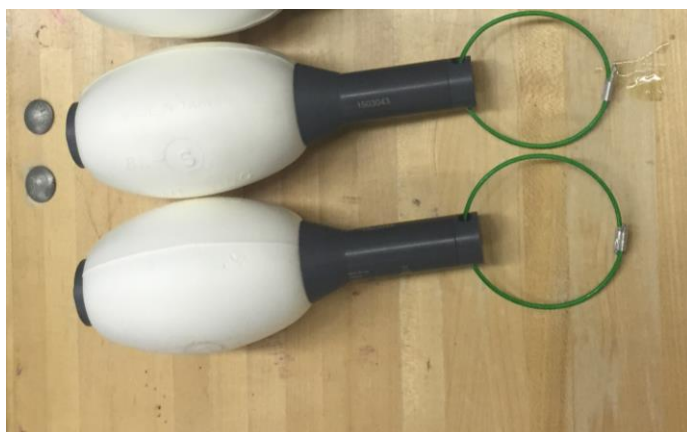


Figure 4. TCM tether

The TCM is secured to the paving stone using a 1/16-inch cable looped through the paving stone and then crimped with a shackle to prevent pull through (Figure 3a). The shackle provides quick accessibility to the instrument by being able easily remove the TCM from the pod to offload data. The length of the TCM tether is restricted to under 2.5 inches to reduce instrument vibrations (Figure 4).

The position of the instrument ensures that the sensor will not move vertically during an event, which will skew the sensor's pressure readings. A secondary anchor rope is looped through the last hole in the concrete base and attached to a 50 pound iron anchor to provide insurance that the entire system will not be lost completely during inundation.

CHAPTER III

RESULTS & DISCUSSION

Wave flume testing

The prototype instrument pod was initially tested in a laboratory wave flume to observe how the system behaves in shallow water under wave attack within a controlled environment (Figure 5).

The TCM continuously recorded at 16 Hz (the optimal setting for short-term deployments

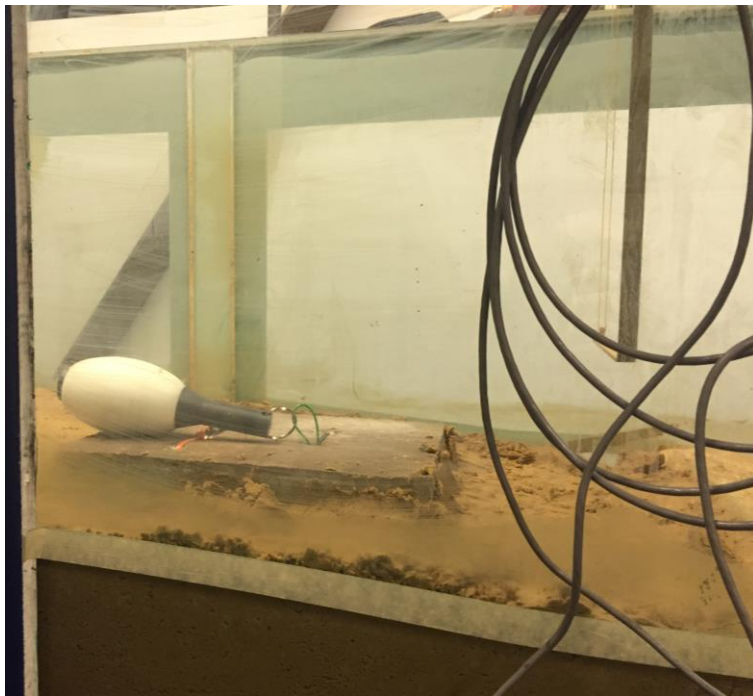


Figure 5. Instrument pod in wave flume prior to testing

according to the manufacturer) while the pressure transducers recorded at 1 Hz (the maximum sampling interval for the HOBOS). The ultimate goal for the RBR solo is to capture not only changes in water surface elevations but resolve infragravity waves (frequencies greater than or equal to 0.0037 Hz and less than 0.05 Hz) as they move the most sediment. However, the wave flume can only simulate waves with a maximum frequency of 0.33Hz. Thus, the minimum

sampling frequency required to properly capture the simulated waves within the wave flume is 1Hz, which is also the maximum sampling rate of the HOBO pressure sensor. It should be noted that each instrument's sampling interval is limited by battery capacity. The battery life for the TCM collecting data continuously at a frequency of 16 Hz is approximately 4.5 months, which is more than adequate to capture an inundation event. The HOBO pressure transducers only have a battery capacity of around six hours with a sampling at a rate of 1Hz, so these instruments are not acceptable for long term deployments. The RBR solo has an estimated 150 days of battery life at 1Hz frequency, perfectly suitable for long deployments.

The wave frequency and water depth were varied over 25 wave flume trials to assess the fidelity of the instrument design as well as the operating limits of the TCM and pressure transducers. However, it should be noted that under this approach, the TCM is being tested beyond its intended use in that the wave flume does not simulate currents but rather orbital wave velocities. Water surface elevations and orbital wave velocities recorded by the pressure transducers and TCM were compared to capacitance wave gauge and a high-resolution acoustic velocimeter data. The capacitance wave gauge measures changes in capacitance at the water surface and then converts and records the data as voltage. The voltage time series for each trial is then converted to a water surface elevation during post-processing using calibration techniques. The Vectrino, a 3D acoustic velocimeter, uses the Doppler Effect to measure current velocity. The Vectrino measures the travel-time of a transmitted pulse after it is reflected by suspended sediment which is assumed to be moving at the same speed as the water.

The first 12 trials kept wave frequency and type (regular) constant while incrementally increasing water levels until the TCM became completely buoyant under static conditions. This approach allowed for us to assess if the TCMs could still capture orbital wave velocity trends

below the minimum water surface elevation as well as identify this threshold. The remaining trials varied wave frequency and type (regular and irregular) while keeping water level constant.

Pressure Sensors

Figure 6 depicts the pressure transducer time series for each instrument over the two-day time period of flume testing. Each trial is signified by a single wave train lasting 120 seconds. All pressure measurements were corrected for atmospheric pressure and are shown below in units of decibars, which serve as a convenient measure of depth in shallow water. Figure 6 shows that there are differences in resolution between the two pressure sensor brands as well as between mounting locations. Both HOBO instruments exhibit oscillations during “still” conditions when the flume was inactive which we interpret as background noise.

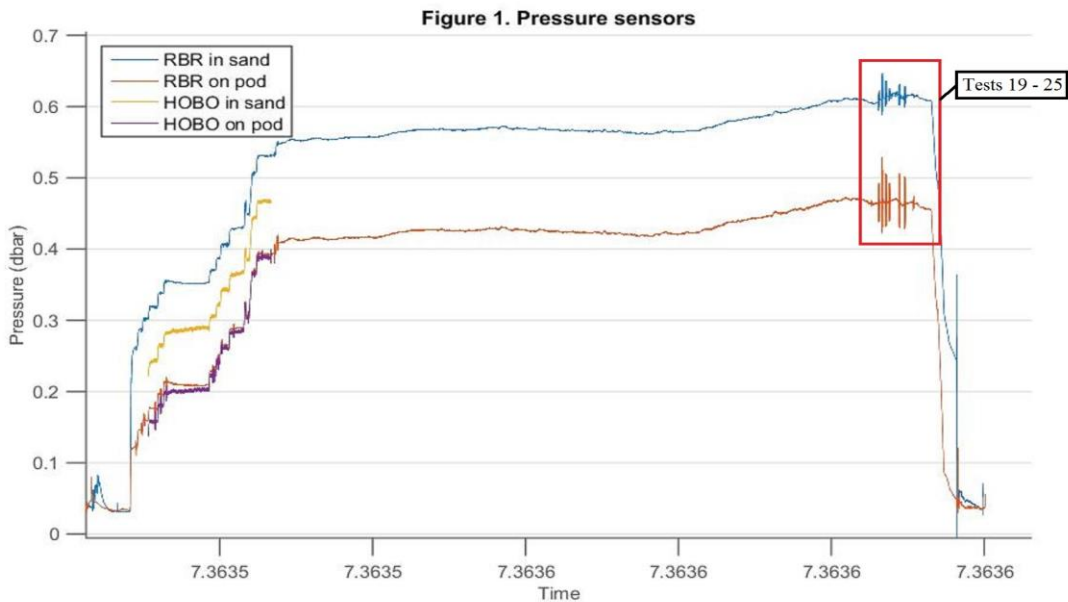


Figure 6. Pressure time series for flume trials

In addition, the dynamic pressure signal appears damped for the sensors that were buried in sand as harmonics are not discernable between still-water conditions. As previously mentioned, this result was expected from the solution of a pressure field at the free surface according to linear

wave theory: the dynamic pressure decays as a function of hyperbolic cosine with increasing depth. However, both sensor brands can resolve hydrostatic changes in pressure as evident through the increase in still-water surface elevations for the first 12 trials. The differences in the media densities (sand versus water) will also play a role in attenuating the dynamic pressure. The trials outlined by the red box are included in further analysis.

After the first day of testing, the water level was gradually increased to a distance of 30.105 cm above the bed for the final seven tests; reflected in Figure 6. Table 1 displays the wave conditions for four wave flume trials highlighted by the red box in Figure 6. These trials were selected for their diversity in simulated wave type, frequency, and height.

Table 1. Wave characteristics of selected flume trials

Test #	Wave Height	Wave Period (s)	Water Level (cm)
20	0.12	1.6	30.105
21	0.06	2.4	30.105
22	0.03	3.2	30.105
25	Nonlinear	1.25	30.105

Data captured by the TCM and the RBR pressure transducers from these four trials are evaluated below.

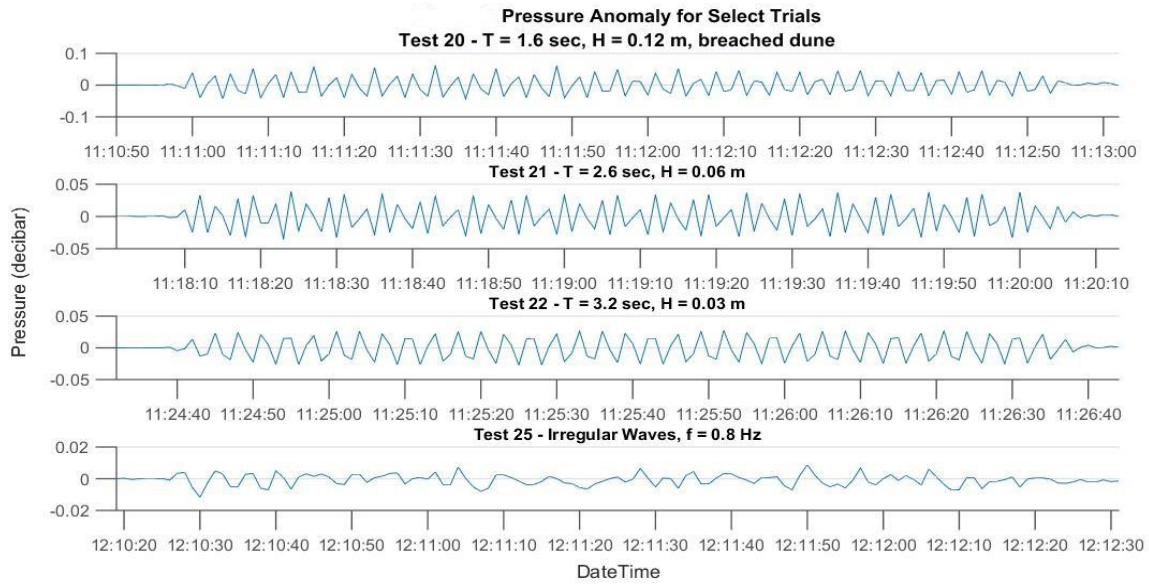


Figure 7. Pressure Anomaly for four flume tests

Figure 7 shows normalized pressure data from the RBR pressure sensor attached to the instrument pod for the four wave flume trials (outlined by the red box in Figure 6). Pressure was normalized by still-water surface elevation for comparison to capacitance wave gauge data.

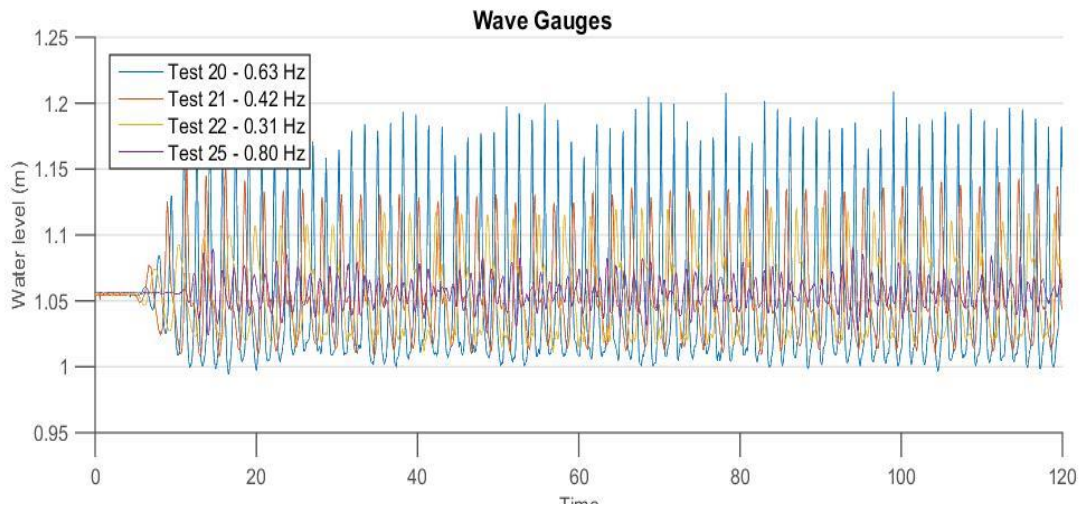


Figure 8. Wave gauge data for four tests

Figure 8 depicts the wave gauge data, including initial still-water levels, for the four trials detailed above. Pressure data was manually discretized to match capacitance gauge data which was not recorded with a time stamp. Precise correlation between the two time series requires detailed numerical analysis which is not discussed herein. The highest resolvable wave frequency for a discrete signal is limited by the Nyquist frequency which for the RBR is 0.5 Hz given a sampling rate of 1 Hz. As visible in Figure 9, this criteria was only met for Test 21 and 22 (0.38 Hz and 0.313 Hz, respectively) and as expected, these signals match well with the frequency of recorded capacitance wave gauge data. The pressure sensor measurements appear to best match the wave gauge frequency for Test 22.

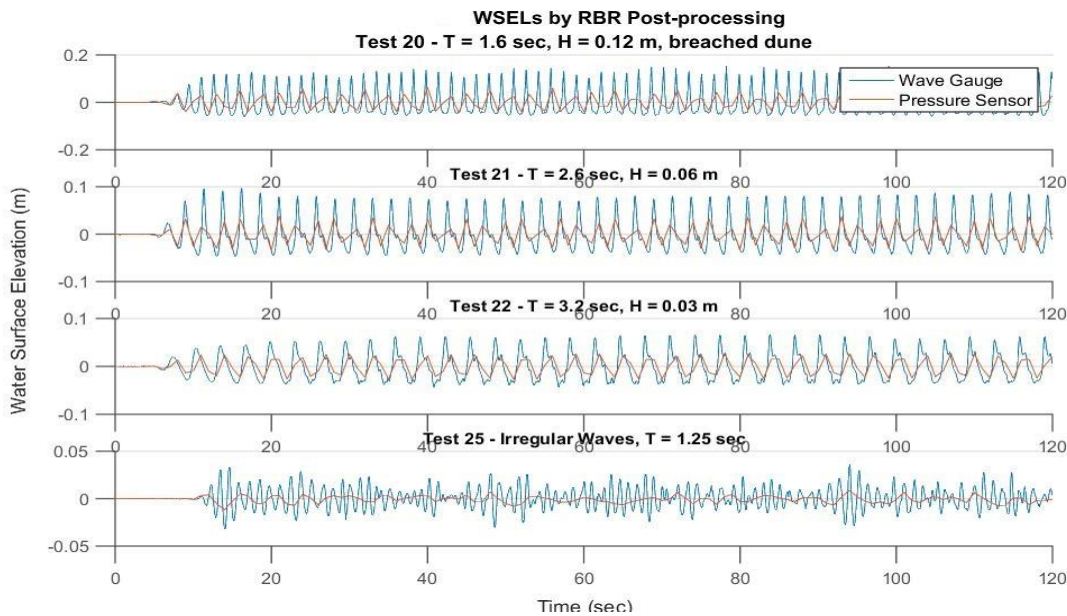


Figure 9. Wave gauge and pressure plot

However, for Test 22 the amplitude is underestimated by the pressure sensors. We interpret this discrepancy as the result of 1) a low sampling rate, 2) smoothing of the waveform due to a damped instrument impulse response for the simulated wave frequency, or 3) a limitation of linear wave theory.

TCM

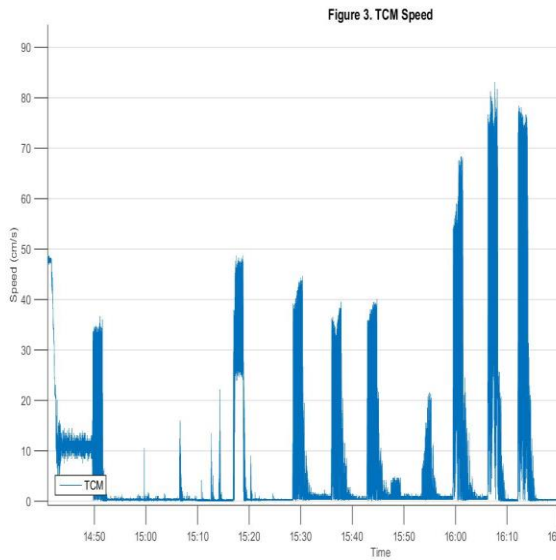


Figure 10a – Raw TCM data Test # 11-18

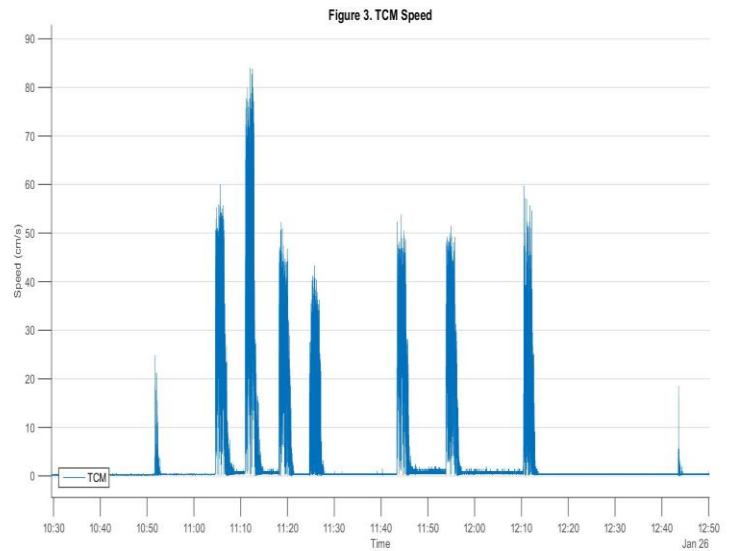


Figure 10b – Test # 19-27

The minimum recommended water level for the TCM to function properly was given as 30cm above the bed. (Chris Sherwood). In this case only the TCM data with a water level between 30cm – 30.105cm were analyzed in Figure 10a and 10b. The date-time axis of 15:14 in Figure 10a corresponds to a wave trial with a water level of 30cm above the bed, wave height of 0.045m and period of 0.8s. The TCM velocity data at Sherwood’s minimum water level in Figure 10a exhibits oscillations only in the positive x direction (direction of the wave) and never returns to its zero position. This may be due a slapping effect caused by the waves as they strike the top of the TCM that is still not fully submerged. This inhibits the TCM from completing its full orbital velocity i.e. move in the negative x direction. When the water level was increased to 30.105m the initial velocity magnitudes approached zero, which is expected when the TCM is motionless. The water level above the bed in Figure 10b is a constant 30.105cm. Over the seven trials the TCM showed consistent velocity data with varying wave height and frequencies. However, the full range of motion of the TCM was still not achieved by observing that the velocity data did not

go below zero. This phenomenon may arise from the fact that the linear waves introduced are not perfectly linear which introduces stokes drift in the direction of the wave.

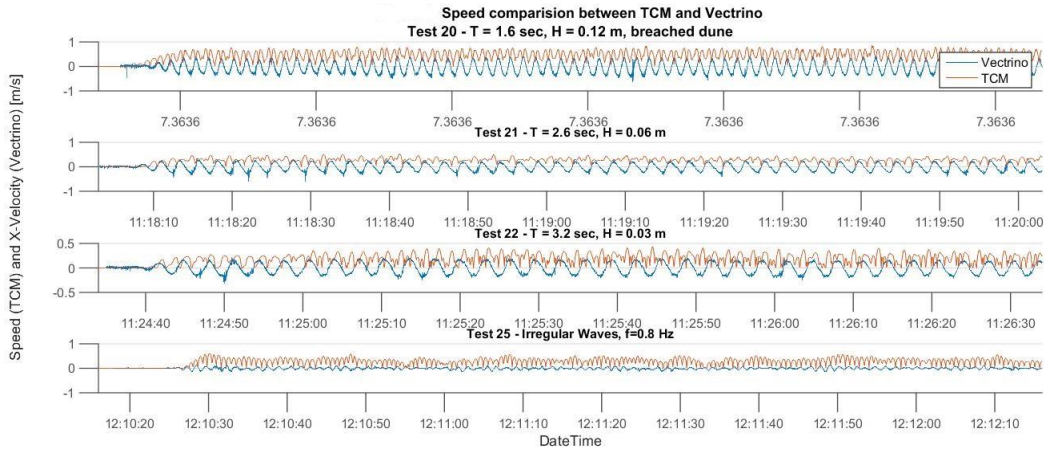


Figure 11 – TCM and Vectrino velocity comparison

Figure 11 represents the wave orbital velocities captured by the TCM and Vectrino in the wave flume at range of wave heights and frequencies. The TCM was able to capture the highest frequency wave and wave height orbital velocities with the greatest accuracy when compared to the Vectrino in Test 20. In Test 21 and 22, the TCM displays turbulent behavior supported by observations of the TCMs erratic movement during the tests. These anomalies in the TCM’s velocity data in the negative and positive direction of the wave may be due to interference by wave reflection in the wave flume that prevent the TCM from completing its oscillatory motion. . In each test, the TCM velocities are offset by some degree relative to the Vectrino data. The irregular wave test produced sporadic velocity results, therefore further testing is needed to study TCM behavior when introduced to an irregular wave.

Preliminary Field Trials

In order to examine the behavior of the instrument setup in a near inundation environment, two instrument pods were deployed for ten minutes in the surf zone off of a local beach in Galveston. Similar to the flume trials, the experiment setup included an acoustic velocimeter, the Nortek Vector (similar to the Vectrino), which provided a reasonable comparison of current velocities to the TCM. The full set up is shown in Figure 12.



Figure 12. Field trial setup

The instrument pods were deployed on either side of the Vector parallel to the beach to capture the long shore drift as well as any cross-shore current. At the deployment site, a strong northeast directed long-shore current was observed which coincided with a peak incoming tide. During instrument retrieval, significant scouring was observed around the concrete paving stones measuring approximately 6 to 12 inches. This rapid scouring may be concerning in that

instrument burial will impede current data collection. Future field trials will seek to address burial erosion concerns through extended deployments and potentially modifications to the instrument pod design. While data processing of the initial field trial are ongoing, preliminary analyses of the pressure sensor and TCM data are included in Figures 13 and 14 below.

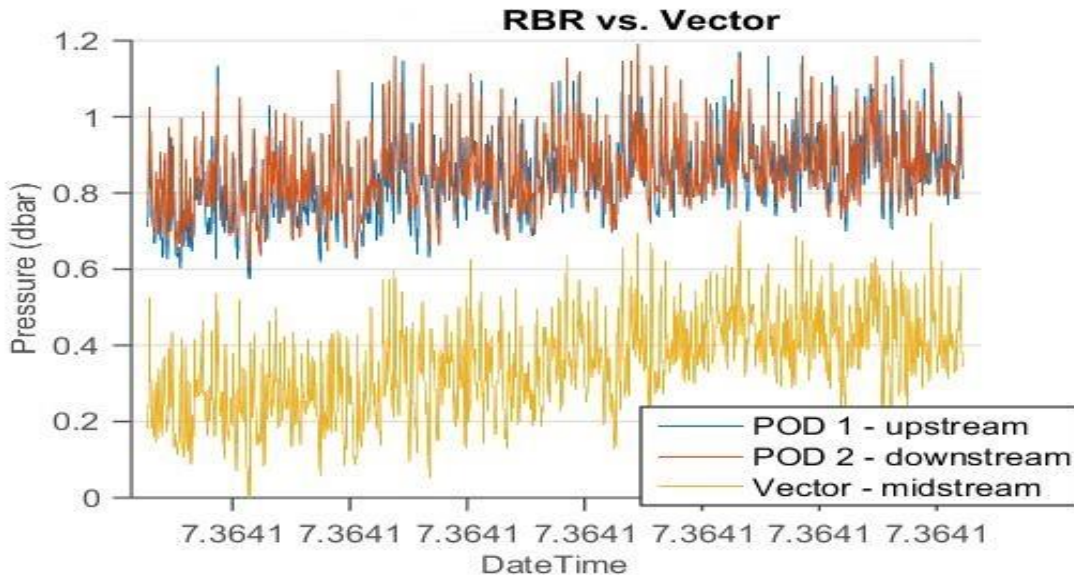


Figure 13. RBR vs. Vector pressure data

The pressure sensors capture the incoming tide as an increase in water level with time (Figure 13). The trend in water levels appear to agree well between the two instrument pods, however further analysis will seek to quantify the correlation between the two instruments pods and the Vector pressure sensor data located. Note that the difference in absolute water levels between the Vector and the instrument pods is due to the Vector’s mounting device which sits approximately 30 inches above the seafloor.

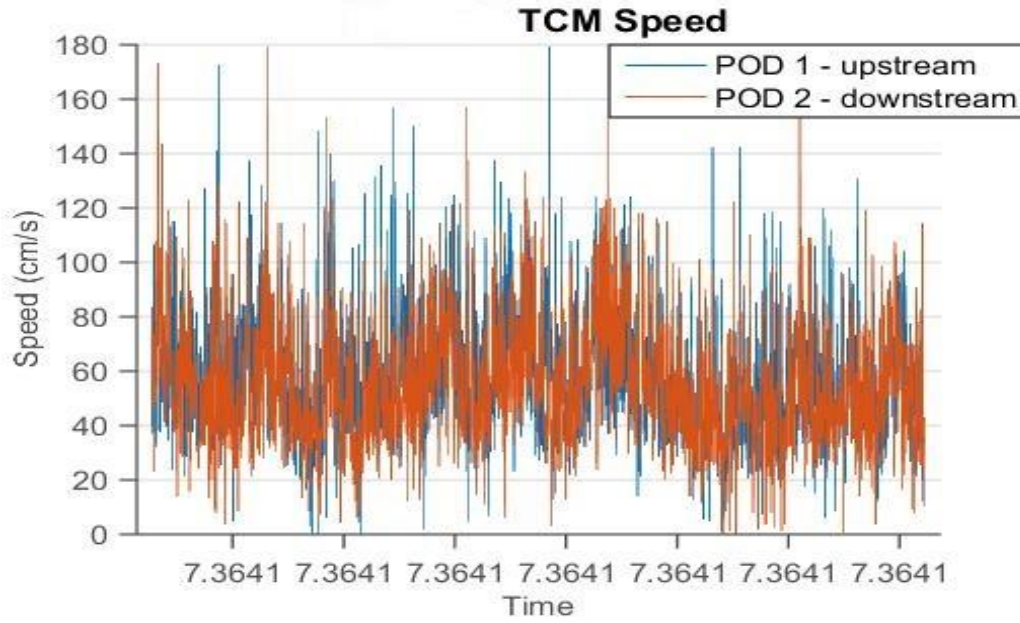


Figure 14. Raw TCM data

Figure 14 displays the current velocity captured in the surf zone. The max velocities recorded by the two pods at around 1.7 m/s are relatable to the strong currents observed while retrieving the instruments.

CONCLUSION

The work presented in this thesis investigates the feasibility of using a new tilt current meter and pressure sensor combination to measure overland flow dynamics in the field during tropical storms or hurricane conditions. The specific goal of this thesis was to develop the most optimal instrument mounting setup, pod design, and anchoring system to survive extreme field conditions during future storm deployments on shallow barrier islands. Furthermore, the capabilities of the various instruments to measure water level, flow velocity, and waves were tested in a wave tank as well as under non-storm field conditions in the surf zone.

Results indicate that the developed system may require further optimization in terms of pod design to minimize scouring during deployment. Furthermore, wave flume tests revealed that the TCM system cannot resolve short period wind waves due to recording frequency and inertia of the float portion of the TCM. The utilized pressure sensors are capable of recording at 2 Hz maximum frequency which is detailed enough to resolve the main low frequency wave motions but not all the high frequency wind waves. While this may be acceptable during a field deployment, it may be worthwhile to replace the pressure sensors with ones capable of recording at higher frequencies.

In general, the system seems robust enough to withstand field deployment and should be capable of producing valuable information of in-situ hydrodynamics during the complex overland barrier island flows generate during storms. Further testing and optimization of the equipment will continue to be ready for the next storm to impact the Upper Texas Coast.

REFERENCES

SALLENGER, A.H., Jr. 2000. Storm Impact Scale for Barrier Islands. *Journal of Coastal Research*, 16(3), 890-895, WestPalm Beach (Florida) ISSN 0749-0208.

Sherwood, C. R., J.W. Long, P. J. Dickhudt, P. S. Dalyander, D. M. Thompson, and N. G. Plant (2014), Inundation of a barrier island (Chandeleur Islands, Louisiana, USA) during a hurricane: Observed water-level gradients and modeled seaward sand transport, *J. Geophys. Res. Earth Surf.*, 119, 1498–1515, doi:10.1002/2013JF003069.

RBR-Global. (2012). *RBRsolo Manual*. Retrieved from http://www.rbr-global.com/component/docman/doc_view/68-ruskin-rbrsolo-user-guide.

Lowell Instruments, LLC. (2014). *Universal User Guide for the TCM-1 Current Meter, MAT-1 Data Logger and MAT Logger Commander Software*. Retrieved from <http://www.lowellinstruments.com>.